SUPPLEMENTARY INFORMATION

Yuanyu Gu,[a,b] Marie Yoshikiyo,[c] Asuka Namai,[c] Debora Bonvin,[d] Abelardo Martinez,[e] Rafael Piñol,[a] Pedro Téllez,[f] Nuno J.O. Silva,[g] Fredrik Ahrentorp,[h] Christer Johansson,[h] Joaquín Marco-Brualla,[i] Raquel Moreno-Loshuertos,[i] Patricio Fernández-Silva,[i] Yuwen Cui,[b] Shin-ichi Ohkoshi,[c] and Angel Millán[a,]*

[a] Instituto de Ciencia de Materiales de Aragón, ICMA-CSIC/University of Zaragoza, C/ Pedro Cerbuna 10, 50006 Zaragoza (Spain)

[b] School of Materials Science and Engineering. Nanjing Tech University, 210009, Nanjing PR China

[c] Department of Chemistry, School of Science, The University of Tokyo, 7-3-1 Hongo, Bunkyo-ku, Tokyo 113-0033, Japan

[d] Powder Technology Laboratory, Institute of Materials, Ecole Polytechnique Fédérale de Lausanne, 1015 Lausanne, Switzerland

[e] Departamento de Electrónica de Potencia. I3A. Universidad de Zaragoza 50018 Zaragoza (Spain)

[f] Servicio de Apoyo a la Investigación. University of Zaragoza, C/ Pedro Cerbuna 10, 50006 Zaragoza (Spain)

[g] Departamento de Física and CICECO, Universidade de Aveiro, 3810–193 Aveiro (Portugal)

[h] RISE Research Institutes of Sweden, 411 33 Göteborg, Sweden

[i] Departamento de Bioquímica, Biología Molecular y Celular, and Instituto de Biocomputación y Física de Sistemas Complejos. University of Zaragoza, C/ Pedro Cerbuna 10, 50006 Zaragoza (Spain)

*Correspondence to: amillan@unizar.es

1. Materials

Copper dichloride ($CuCl_2$, 99.999%), methyl 2-chloropropionate (MCP, 97%), Formic acid (88 %), Formaldehyde (37% in water), triethylamine (Et_3N, 99%) Triethylenetetramine (tren, 97%), Rodhamine B (95%), N,N-dimethylaminopyridine (DMAP, 98%), Dicyclohexylcarbodiimide (DCC, 99%) were supplied by Sigma Aldrich and used as received. 4-vinyl pyridine (4VP, Aldrich, 95%) was distilled under vacuum and stored at -5ºC . Copper chloride (CuCl, Aldrich) was purified with acetic acid, filtered, washed with ethanol and diethyl ether, and stored under vacuum. Methoxypoly(ethylene)glycol acrylate (MPEGA, Mn=480 Da, Aldrich) was filtered through a pad of neutral alumina before use. Commercially available Polyethylenglicolmethacrylate (PEGMA, Mn: 360Da, Aldrich) was purified following refs [1] and [2]; (Mn: 438 Da, calculated by NMR after purification). Tris [(2-pyridyl) methyl] amine (TPMA) and Tris[2-(dimethylamino)ethyl]amine (Me6-tren) were prepared as reported in [3]. The molecular structure and purity of all the polyethylene glycol derivatives used in this work was confirmed by proton NMR spectroscopy (^{1}H-NMR) using $CDCl_3$ as solvent in a BRUKER AV-400 spectrometer (400 MHz). ^{1}H chemical shifts (δ) are reported in ppm and are referenced to the solvent peak, the coupling constants (J) are given in Hz. Purity was additionally checked by mass spectroscopy (MALDI TOFMS) using dithranol (DTH) as matrix and sodium trifluoroacetate (NaTFA) as cationization agent in a BrukerMicroFlex spectrometer.

2 Synthesis of the polymers

2.1 Synthesis of Rodhamine-polyethylenglycolmethacrylate, ***Rod-PEGMA***

To a solution of PEGMA (5.70 g, 12.5 mmol) in dry dichloromethane (50 mL), Rhodamine B (4.79 g, 10 mmol), DMAP (125 mg, 1 mmol) and a few crystals of 2,6-di.tert-butyl-4-methylphenol were added under argon atmosphere. The solution was cooled into an ice-water and DCC (2.08 g, 10 mmol) were added. Mixture was allowed to reach room temperature and stirred overnight. Solid was filter off and solvent was evaporated under vacuum. The crude product was dissolved in saturated sodium bicarbonate (100 mL). The aqueous phase was washed several times with ethyl acetate, saturated with sodium chloride and extracted several times with a mixture of dichloromethane/2-propanol (3:1) until a clear aqueous phase was observed. The combined organic phases were dried over

magnesium sulphate and concentrated under vacuum. Purification of the final compound was performed by flash chromatography in silicagel using a mixture of ethyl acetate/methanol (7:3) and Et_3N (99:1, v:v) as eluent. 4.96 g (yield: 55%) of a purple sticky solid was obtained. Mn (NMR): 942 g/mol.

^{1}H-RMN ($CDCl_3$, δ ppm): 8.32 (dd, J_1: 7.84 Hz, J_2: 0.95 Hz, 1H), 7.83-7.77 (m, 1H), 7.75-7.70 (m, 1H), 7.28 (dd, J_1: 7.57 Hz, J_2: 0.95 Hz, 1H), 7.05 (d, J: 9.48 Hz, 2H), 6.87 (dd, J_1: 9.50 Hz, J_2: 2.38 Hz 2H), 6.80 (d, J. 2.38, 2H), 6.097 (s, 1H), 5.55 (s, 1H), 4.30-4.24 (m, 2H), 4.17 (t, J: 4.64 Hz, 2H), 3.77-3.49 (m, 32 H), 2.30 (br, s, 8H), 1.91 (s, 3H), 1.31 (t, J: 7.08, 12H).

2.2 Synthesis of poly(4-vinylpyridine)-block-poly(methoxypolyethylenglycolacrylate-co-Rhodamine polyethylenglycolmethacrylate-co-carboxylic polyethylenglycolmethacrylate), ***P4VP-b-P(MPEGA-co-RhodPEGMA-carboxylicPEGMA****.*

Block copolymer P4VP-b-P(MPEGA-co-RhodPEGMA-carboxylicPEGMA used for the coating of iron oxide nanoparticles was prepared by atom transfer radical polymerization (ATRP) according to methods described elsewhere [3]. A scheme is shown in Fig 1S. The synthesis and characterization of the macroinitiator P4VP-Cl has already been published in the above mentioned references.

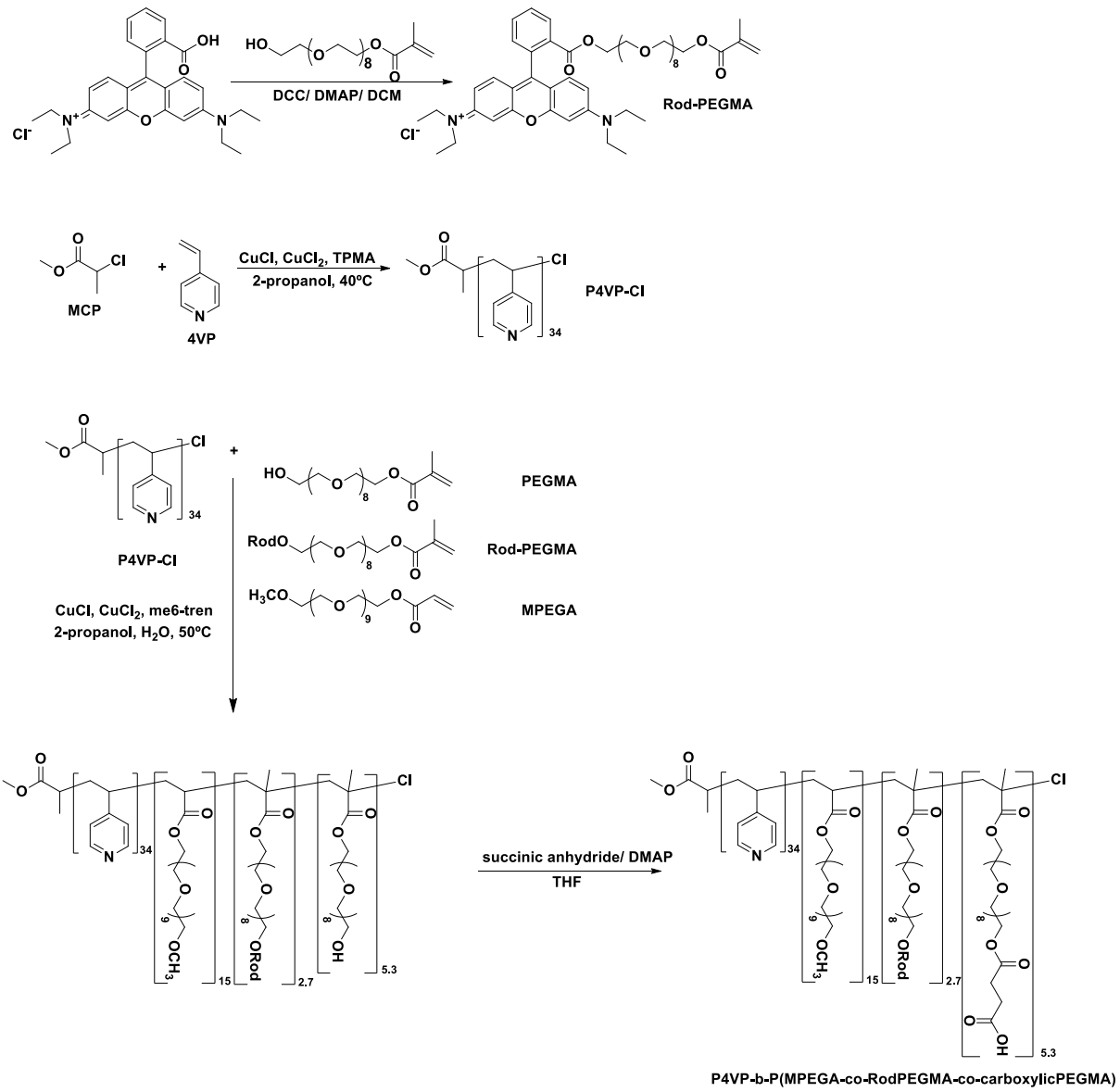

Fig. S1. Synthetic route for P4VP-Cl and P4VP-b-P(MPEGA-co-RhodPEGMA-co-carboxylic PEGMA).

2.2.1. Synthesis of ***P4VP-b-P(MPEGA-co-RhodPEGMA-co-PEGMA).***

In a typical synthesis a 50 mL Schlenk flask with a magnetic stir bar was charged with P4VP-Cl (1.84 g, 0.50 mmol), MPEGA (4.6 mL, 10.5mmol), PEGMA (1.2 mL, 3 mmol), Rhod-PEGMA (1.4 g, 1.5 mmol), Me6-Tren (134 µL, 0.50 mmol) and 16 mL of a mixture of H_2O:2-propanol (1:1). The mixture was frozen in liquid nitrogen and degassed by three freeze-pump-thaw cycles. Then the flask was filled with argon and CuCl (34.65 mg, 0.35 mmol) and CuCl2 (20.17 mg, 0.15 mmol) was added while the mixture was still frozen. The flask was sealed again, purged by three short vacuum-argon and then immersed in an

oil bath thermostated at 50ºC. After 3 hours the flask was open to the atmosphere and mixture was cooled to room temperature. Reaction mixture was poured into a large volume of cold diethyl ether. The crude product was dissolved in 50 mL of dichloromethane, and the organic phase was washed twice with 25 mL of distilled water and 25 mL of brine and dried over magnesium sulfate. 0.35 g of DOWEX® Marathon MSC (Na) ion-exchange resin was added to the polymer solution and the mixture was stirred for 1 hour minutes at room temperature. Resin was filtered off and solvent evaporated under vacuum. The block copolymer was dissolved in methanol and filtered through a pad of silicagel, concentrated under vacuum, purified twice by dissolving in diclorometh ane and precipitation in a large volume of cold ether and finally dried by freeze drying. 3.9 g of polymer was obtained. The percentage conversion and the corresponding degree of polymerization (DP) of each monomer ((MPEGA, 70%, DP:15), (Rhod-PEGMA, 90%, DP:2.7), (PEGMA, 90%, DP: 5.3)) and number average molecular weight of the polymer (Mn(NMR): 15755 Da) were determined by ^{1}H-NMR.

2.2.2. Synthesis of ***P4VP-b-P(MPEGA-co-Rod PEGMA-co-carboxylicPEGMA)***

To a solution of P4VP-b-P(MPEGA-co-Rod PEGMA-co-PEGMA) (3.7 g, 1.25 mmol (-OH)) in dry tetrahydrofuran (25 mL), DMAP (15 mg, 0.125 mmol) and succinic anhydride (250 mg, 2.5 mmol) were added under argon atmosphere. The mixture was stirred at room temperature for 24 hours, salts were filtered off and solvent evaporated under vacuum. Polymer was purified twice by dissolving in small volume of diclorometh ane and precipitation in a large volume of cold ether and finally dried by freeze drying. 3.1 g of polymer was obtained. (Yield: 84%, Mn(NMR): 16250 Da.)

3 X-ray powder diffraction

Comparison of XRD pattern of ε-Fe_2O_3 sample with α-Fe_2O_3, and γ-Fe_2O_3 calculated patterns.

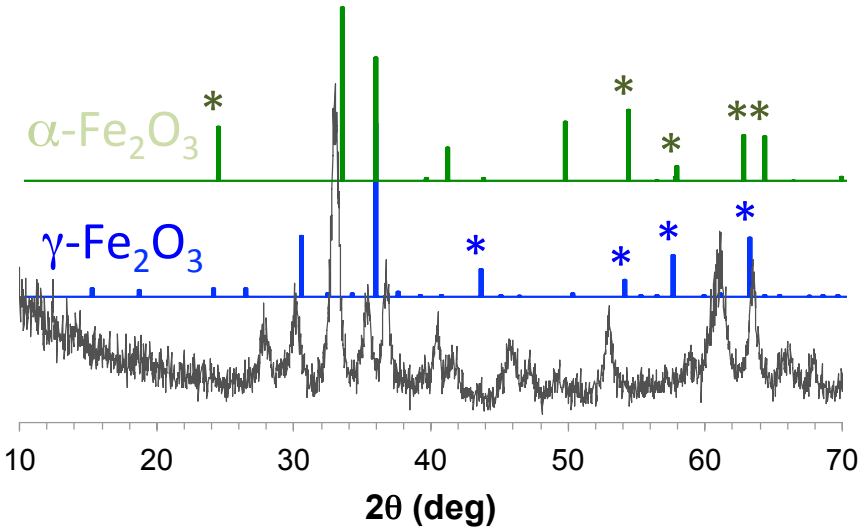

Fig. S2. XRD powder diffraction pattern of the sample in comparison with α-Fe_2O_3, and γ-Fe_2O_3, crystal structure simulated patterns in the ICSD database. Significant α-Fe_2O_3 and γ-Fe_2O_3 reflections (marked with an asterisk) do not appear in the sample pattern demonstrating the absence of these phases in the sample.

4. DLS Measurements

Analysis of the NP suspensions was performed by Dynamic Light Scattering. The obtained values of average hydrodynamic diameter, D_H, polydispersity (PDI) and Z-potential values are presented in Table S1. Plots of the intensities distribution are shown in Figure S3.

Table S1. Average size by number (D_H) , polydispersity (*PDI*) and Zeta potential results of the of the NP suspension samples.

Sample	D_H (nm)	Z-potential (mV)	PDI
ε-Fe_2O_3 uncoated	18	-40.2	0.144
ε-Fe_2O_3 coated	27	-38.9	0.131
γ-Fe_2O_3 uncoated	29	36.0	0.189
γ-Fe_2O_3 coated	36	-13.7	0.158

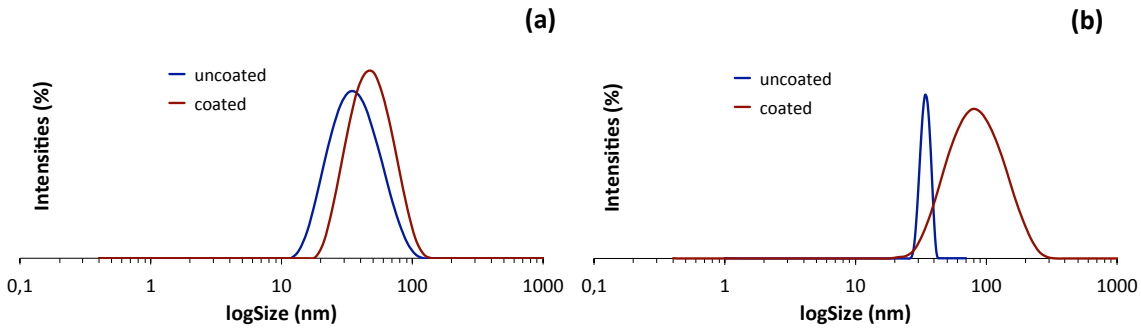

Fig. S3. Dynamic light scattering (DLS) intensity plots of coated and uncoated ε-Fe_2O_3 NPs and (d) γ-Fe_2O_3 NPs.

4 AC Magnetic susceptibility vs temperature

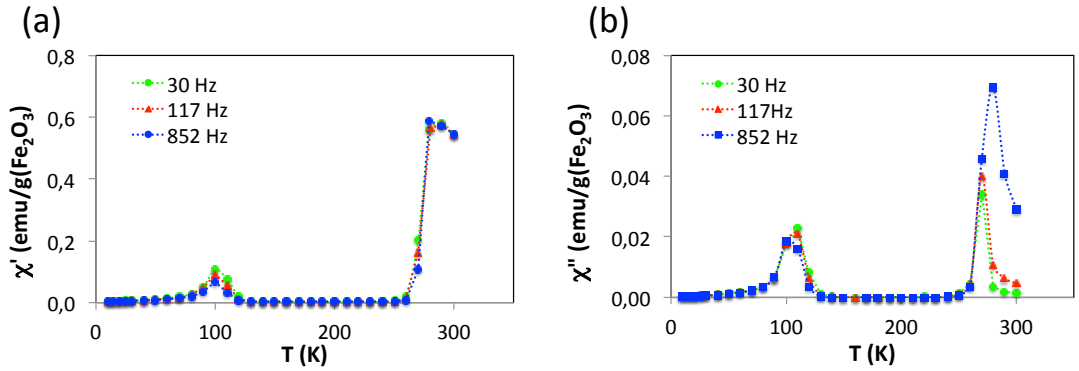

Fig. S4. Temperature dependence of the in-phase (**a**) and out-of-phase (**b**) ac magnetic susceptibility of e-Fe_2O_3 uncoated NP suspension.

5 SAR vs H plots

The variation of *SAR* with the amplitude of the magnetic field, *H*, is shown in Fig S5. In the low frequency range, ε-Fe_2O_3 and g-Fe_2O_3 NPs showed comparable *SAR* values (Fig S5(a)&(b)). The SAR increased linearly with the field amplitude, *H*. For the other frequencies, SAR vs H curves had a more exponential shape, at some of the used frequencies, for both types of NPs. For ε-Fe_2O_3 NPs, the slope of the *SAR* vs *H* curves (Fig S5(a)) was increasing with the frequency in the range from 25 to 61 kHz, and they overlapped after that. For the γ-Fe_2O_3 NPs, the slope of the SAR vs H curves (Fig 2(b)) was continuously increasing with the frequency in the whole measurement range (26-90 kHz). In the high frequency range (400 kHz to 800 kHz) ε-Fe_2O_3 and γ-Fe_2O_3 NPs followed opposite trends (Figs S5(c)&(d)). The SAR values of ε-Fe_2O_3 NPs dropped to one-half while those of γ-Fe_2O_3 NPs increased by one order of magnitude for a given field amplitude. In addition, the response to frequency is different between the two phases. In ε-Fe_2O_3 NPs, the frequency has only a little impact on SAR for any given field amplitude (Fig S5(c)). But, in γ-Fe_2O_3 NPs, when the frequency increases from 419 kHz to 710 kHz the SAR values doubles. A further increase to 829 kHz does not cause any variation on SAR (Fig S5(d)).

Concerning coated NPs, SAR values decreased with respect to uncoated NPs (Fig. S6(a)&(b)) in the low frequency range, especially in the case of γ-Fe_2O_3 (Fig. S6(b)). However, in the high frequency range, SAR values of coated γ-Fe_2O_3 NPs showed a moderate decrease with respect to the uncoated NPs in the whole measuring range (Fig

S6(d)). But, SAR values of ε-Fe_2O_3 NPs dropped drastically after coating, especially at the highest frequencies (Fig S4(c)).

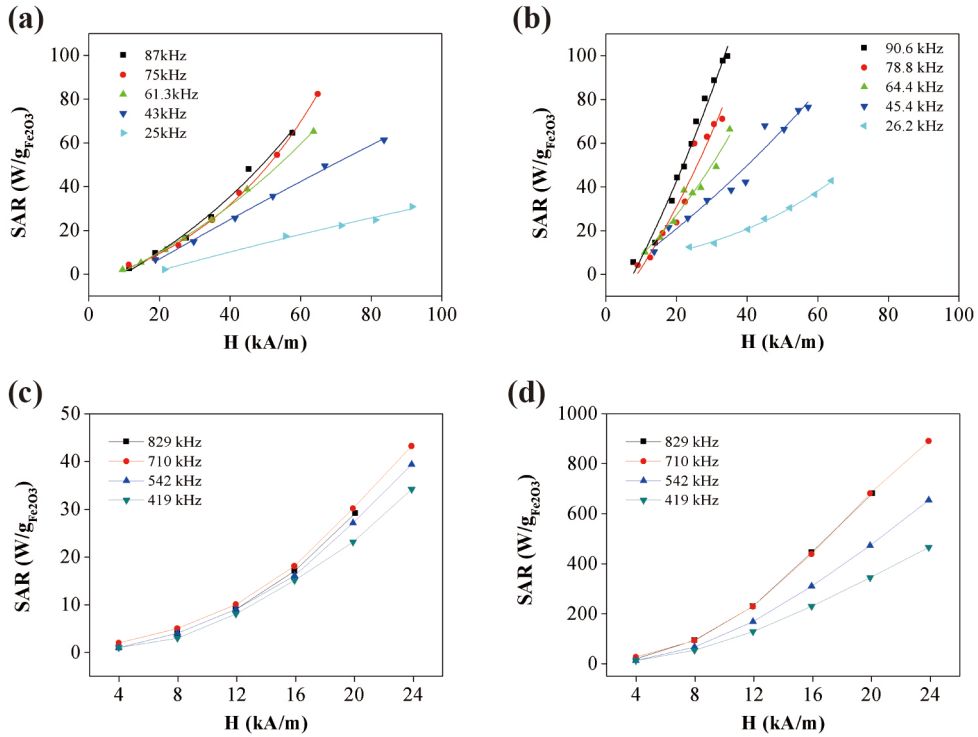

Fig. S5. SAR values as a function of magnetic field amplitude *H* of aqueous suspensions of: (**a**) uncoated ε-Fe_2O_3 NPs and (**b**) uncoated γ-Fe_2O_3 NPs, in the low frequency range; (**c**) uncoated ε-Fe_2O_3 and (**d**) uncoated γ-Fe_2O_3 NPs, in the high frequency range. Solid lines are guides to the eye.

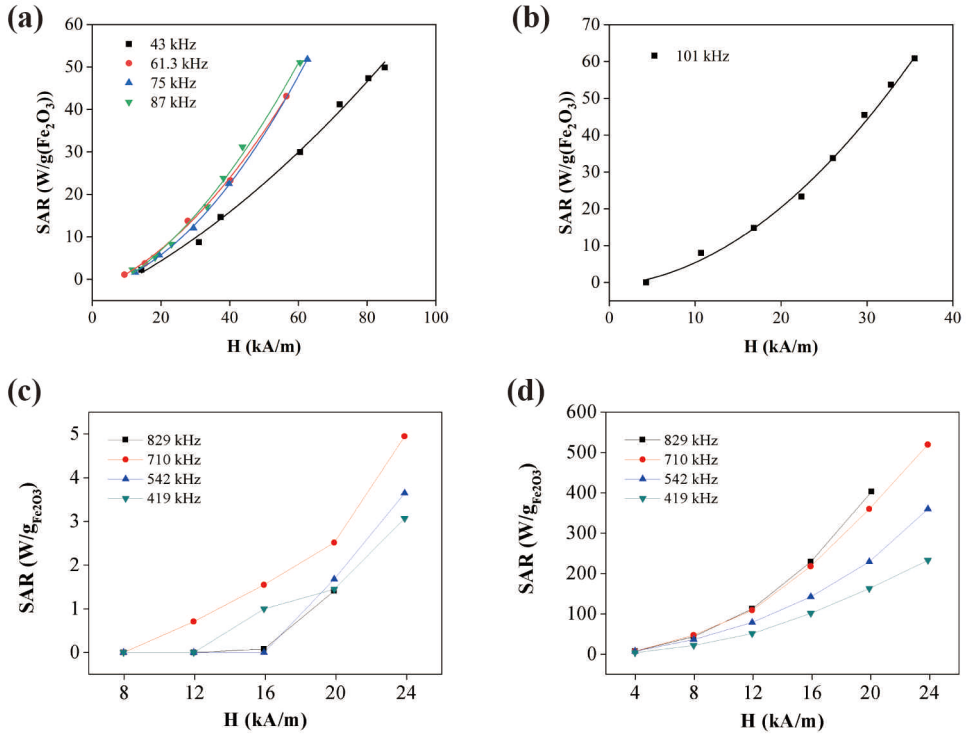

Fig. S6. SAR values as a function of magnetic field amplitude *H* of aqueous suspensions of: (**a**) polymer coated ε-Fe_2O_3 NPs and (**b**) polymer coated γ-Fe_2O_3 NPs in the low frequency range; and

(**c**) polymer coated ε-Fe_2O_3 and (**d**) polymer coated γ-Fe_2O_3 NPs, in the high frequency range. Solid lines are guides to the eye.

References

1. J. Klier, A. B. Scranton, N. A. Peppas, Self-associating networks of poly(methacrylic acid-G-ethylene glycol), *Macromolecules*, 1990, **23**, 4944-4949.
2. M. M. Ali, H. D. Stöver, Well-defined amphiphilic thermosensitive copolymers based on poly (ethylene glycol monomethacrylate) and methyl methacrylate prepared by atom transfer radical polymerization, *Macromolecules*, 2004, **37**, 5219-5227.